Mon. Not. R. Astron. Soc. **000**, 1–9 (2011) Printed 25 October 2011 (MN LaTeX style file v2.2)

The *XMM-Newton* view of supergiant fast X–ray transients: the case of IGR J16418–4532

L. Sidoli,[1⋆] S. Mereghetti,[1] V. Sguera,[2] and F. Pizzolato,[1]
[1]INAF, Istituto di Astrofisica Spaziale e Fisica Cosmica, Via E. Bassini 15, I-20133 Milano, Italy
[2]INAF, Istituto di Astrofisica Spaziale e Fisica Cosmica, Via Gobetti 101, I-40129 Bologna, Italy

Accepted 2011 October 23. Received 2011 October 18; in original form 2011 August 29

ABSTRACT

We report on a 40 ks long, uninterrupted X–ray observation of the candidate supergiant fast X–ray transient (SFXTs) IGR J16418–4532 performed with *XMM-Newton* on February 23, 2011. This high mass X–ray binary lies in the direction of the Norma arm, at an estimated distance of 13 kpc. During the observation, the source showed strong variability exceeding two orders of magnitudes, never observed before from this source. Its X–ray flux varied in the range from ∼0.1 counts s^{-1} to ∼15 counts s^{-1}, with several bright flares of different durations (from a few hundreds to a few thousands seconds) and sometimes with a quasi-periodic behaviour. This finding supports the previous suggestion that IGR J16418–4532 is a member of the SFXTs class. In our new observation we measured a pulse period of 1212±6 s, thus confirming that this binary contains a slowly rotating neutron star. During the periods of low luminosity the source spectrum is softer and more absorbed than during the flares. A soft excess is present below 2 keV in the cumulative flares spectrum, possibly due to ionized wind material at a distance similar to the neutron star accretion radius. The kind of X–ray variability displayed by IGR J16418–4532, its dynamic range and time scale, together with the sporadic presence of quasi-periodic flaring, all are suggestive of a transitional accretion regime between pure wind accretion and full Roche lobe overflow. We discuss here for the first time this hypothesis to explain the behaviour of IGR J16418–4532 and, possibly, of other SFXTs with short orbital periods.

Key words: X–rays: individual (IGR J16418–4532)

1 INTRODUCTION

IGR J16418–4532 is a transient X-ray source discovered in the direction of the Norma Galactic arm during *INTEGRAL* observations performed on 2003 February 1–5 (Tomsick et al. 2004). Its proposed optical/infrared counterpart (2MASS J16415078–4532253, Chaty et al. 2008, Rahoui et al. 2008), positionally consistent with the accurate localization obtained with the *Swift* X-Ray Telescope (Romano et al. 2011), is indicative of a high mass X–ray binary (HMXB) at a distance of about 13 kpc. The short time interval of X–ray activity observed with *INTEGRAL* suggested to classify IGR J16418–4532 as a supergiant fast X–ray transient (SFXT, Sguera et al. 2006).

Walter et al. (2006) reported the presence of pulsations at 1246±100 s in an *XMM-Newton* observation obtained in 2004, while a periodicity of 3.753±0.004 days (Corbet et al. 2006) or 3.7389±0.0004 days (Corbet et al. 2006, Levine et al. 2011) was obtained from an analysis of the long term light curves from the *Swift* Burst Alert Telescope and the *RXTE* All Sky Monitor data (ASM), respectively. This modulation has been interpreted as the orbital period[1] of the binary system.

Following the MAXI satellite discovery of renewed X-ray activity from the region of IGR J16418–4532 in February 2011 (as reported in Romano et al. 2011), we performed a Target of Opportunity *XMM-Newton* observation. The new *XMM-Newton* data show variability spanning an unprecedented range in this source, thus supporting its SFXT nature. Furthermore, the frequent presence of strong quasi-periodic flares suggests that this long spin-period pulsar in a relatively compact HMXB (as implied by the short orbital period), might be in an intermediate accretion regime between Roche-lobe overflow and wind accretion.

2 OBSERVATIONS AND DATA REDUCTION

IGR J16418–4532 was observed with *XMM-Newton* between 2011 February 23 (at 13:55 UT) and February 24 (at 00:32

⋆ E-mail: sidoli@iasf-milano.inaf.it

[1] the formal discrepancy between the two periods is probably due to an underestimation of the respecive errors.

UT), with a net exposure of about 39 ks. The XMM-$Newton$ $Observatory$ carries three 1500 cm^2 X–ray telescopes, each with an European Photon Imaging Camera (EPIC) at the focus. Two of the EPIC use Metal Oxide Semi-conductor (MOS) CCDs (Turner et al. 2001) and one uses a pn CCD (Strüder et al. 2001). Reflection Grating Spectrometer (RGS) arrays (den Herder et al. 2001) are located behind two of the telescopes.

Data were reprocessed using version 11.0 of the Science Analysis Software (SAS). Both MOS and pn operated in Full Frame mode and used the medium thickness filter. Extraction radii of 40′′ and 1′ were used for the source events, respectively for the pn and MOS cameras. Background counts were obtained from similar sized regions, offset from the source position, and in the same temporal intervals, when dealing with time selected analysis. The background (selected with PATTERN=0 and in the energy range 10–12 keV in the pn) showed evidence of flaring activity only during the first 12 ks of the observation. Therefore, we removed the corresponding time interval in most of our analysis, as discussed in detail in the next section.

Response and ancillary matrix files were generated using the SAS tasks RMFGEN and ARFGEN. Using the SAS task EPATPLOT, we found that MOS spectra were affected by pile-up. Thus, we report here only on EPIC pn spectroscopy (adding MOS data did not improve the spectral fitting), while for the timing analysis both the two MOS and the pn were considered. Spectra were selected using patterns from 0 to 4 with the pn.

To ensure applicability of the χ^2 statistics, the net spectra were rebinned such that at least 30 counts per bin were present and such that the energy resolution was not over-sampled by more than a factor 3. All spectral uncertainties and upper-limits are given at 90% confidence for one interesting parameter. In the spectral fitting we used the photoelectric absorption model PHABS in XSPEC with the interstellar abundances of Wilms et al. (2000). The RGSs were operated in spectroscopy mode (den Herder et al. 2001), but given the high absorbing column density, they did not detect the source.

To better investigate the long term behaviour of IGR J16418–4532 we reanalysed also the 2004 XMM-$Newton$/EPIC observation, first reported by Walter et al. (2006), with the same procedures and selection criteria used for the 2011 data[2].

3 ANALYSIS AND RESULTS

3.1 Spectroscopy

The EPIC pn, background subtracted, light curves of IGR J16418–4532 observed in 2004 and in 2011 are shown in Fig. 1. Letters mark time intervals showing different kinds of X-ray activity within each observation. In particular, strong flares are seen in time intervals B, D, and F, while in the remaining time intervals the source was in a low intensity state, with less frequent and fainter flares. As mentioned above, the first part of the 2011 observation (time interval D) was affected by high background level, so in the following we will not use this time interval, except when extracting the spectra from the peaks of the bright flares (for which the background contribution is negligible).

We first analysed the average spectrum of each observation, corresponding to a net integration time of 19.6 ks for the 2004 data, and 23.8 ks for the 2011 data (intervals E and F). The best fit parameters obtained with an absorbed power law model are listed in Table 1 and the spectra shown in Fig. 2. A similar spectral slope is seen in the two observations, while the absorption in 2011 was about a half of that observed in 2004. While the 2004 spectrum is reasonably well fitted by the power law model (although with marginal evidence for a soft excess below 2 keV), structured wave-like residuals over the entire energy range are evident in the 2011 spectrum, with a positive excess below 2 keV more pronounced than in 2004.

[2] except for the pn source extraction region, for which we adopted a radius of 20′′ to avoid stray light contamination from a bright transient source located outside the field of view.

Table 1. Spectral results of the time averaged spectra of the 2004 and 2011 XMM-$Newton$ observations. An absorbed power law model was used. Γ is the power law photon index. Flux is in the 1–10 keV energy range in units of 10^{-11} erg cm^{-2} s^{-1} and is corrected for the absorption, N_H (in units of 10^{22} cm^{-2}).

Parameter	2004 (A+B+C)	2011 (E+F)
N_H	15 ± 1	7.4 ± 0.3
Γ	1.3 ± 0.1	1.28 ± 0.05
Unabs. Flux	1.8	1.5
χ^2_ν/dof	1.147/166	1.252/210

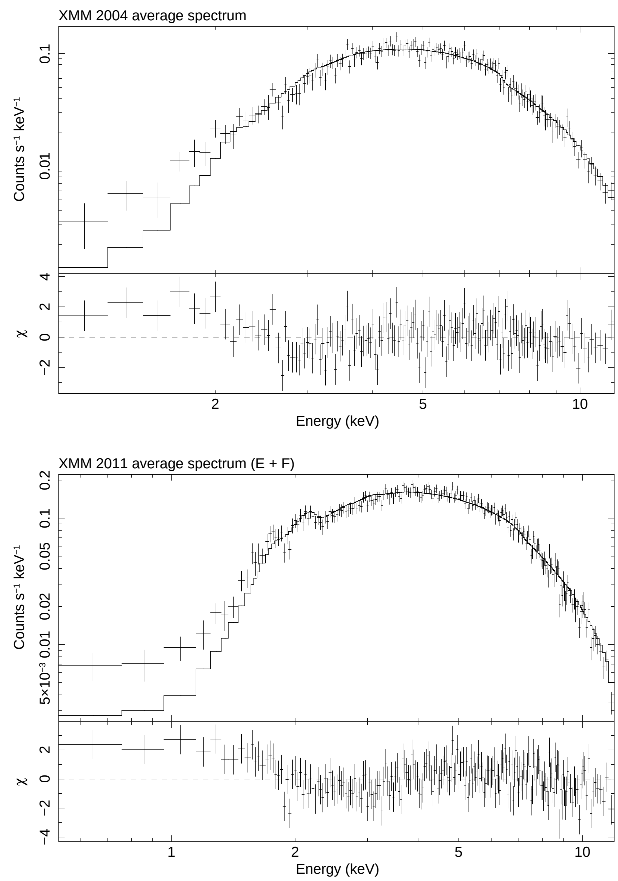

Figure 2. Spectral results of the average spectra extracted from the EPIC pn observations in 2004 (*upper panel*) and in 2011 (*lower panel*). Count spectra are shown, together with the residuals (in units of standard deviations) of the data to the absorbed power law model (Table 1).

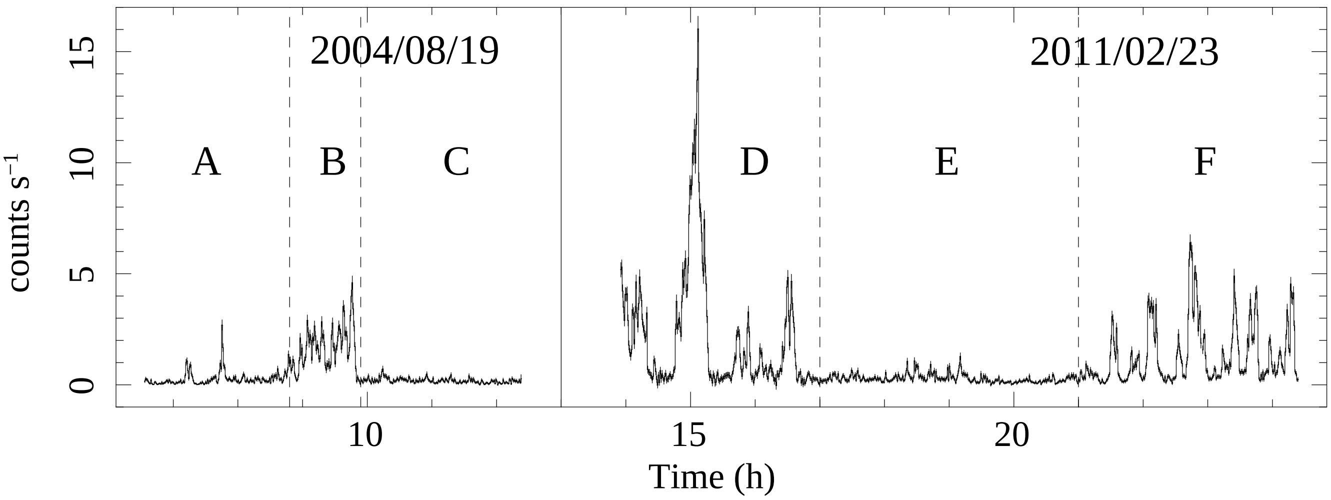

Figure 1. EPIC pn, background-subtracted, light curves of IGR J16418–4532 in the 0.3–12 keV energy range. The bin size is 50 s and the time axis is in UTC hours of the dates indicated in the panels. Letters indicate the different intervals used for the time selected spectroscopy. Note that also during the non-flaring time intervals, the source is significantly detected, with average count rates $0.185{\pm}0.006$ counts s^{-1} and $0.331{\pm}0.005$ counts s^{-1} in 2004 (interval C) and 2011 (interval E), respectively (0.3–12 keV).

We next considered temporal selected spectra, extracting different spectra from the flaring intervals and from the low intensity emission, within each observation.

We first considered the 2004 observation, when IGR J16418–4532 showed a bright flare with a complex shape (interval B, Fig. 1, left panel) in the middle of two low-intensity time intervals (A and C). We extracted a spectrum from each time interval (A, B and C), with the one of interval B formed by selecting only the events corresponding to time intervals with count rate above 0.5 counts s^{-1}. The results for these spectra, fitted with an absorbed power law, are reported in Table 2. We also extracted a further low intensity spectrum from time intervals A and C, but now excluding the two faint flares that occurred in time interval A. This “cleaned A+C” spectrum is indeed more representative of the low intensity emission in 2004. A comparison with the flare spectrum (B) indicates that the IGR J16418–4532 X–ray emission is less absorbed during flares. There is also a possible hint for a flatter spectral slope when the source is brighter, but the uncertainties are too large to draw a firm conclusion, based on the 2004 observation only.

We next considered the observation performed in 2011. In order to investigate the spectral properties of the single flares we selected all time intervals with a count rate above 1 counts s^{-1} in the pn light curve (0.3–12 keV) binned at 256 s. This time selection yielded 16 single flares (6 flares in time interval D and 10 in F). An absorbed power-law gave almost always a good fit to each single flare spectrum. The best fit parameters of each flare are shown in Fig. 3, which shows no evidence for significant spectral variability between the flares, even comparing flares in the first part of the observation (interval D) with those located in the second part (interval F). Most of the flare spectra require an absorption well in excess of the total Galactic value towards IGR J16418–4532 ($1.9{\times}10^{22}$ cm^{-2}, Dickey & Lockman 1990). A black body model always results in a worse (or in an equally good) fit, giving densities, on average, a half of the value obtained with a power law. The black body temperatures are $\sim$2 keV, and the resulting black body radii have values of a few hundred meters at 13 kpc.

We next extracted a cumulative “spectrum during flares” by summing all the spectra of the flares occurring in the time interval

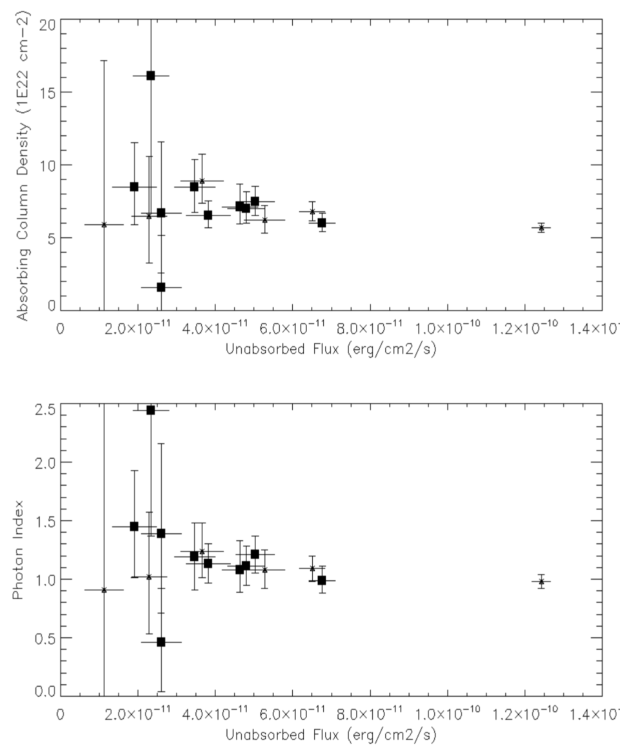

Figure 3. Spectral results of the intensity selected spectroscopy of all flares observed in 2011. The assumed model is an absorbed power law. *Upper panel* shows the absorbing column density evolution with the flux corrected for the absorption, while the *Lower panel* displays the photon index versus unabsorbed flux (1–10 keV). *Light triangles* mark the spectral parameters of the flares extracted from the first part of the 2011 observation (interval D in Fig. 1), while *solid black squares* indicate flares occurred in the second flaring part of the same observation (interval F in Fig. 1).

Table 2. Results of the time selected spectroscopy (letters mark the same time intervals displayed in Fig. 1). An absorbed power law model was used. Flux is in the 1–10 keV energy range in units of 10^{-11} erg cm^{-2} s^{-1} and is corrected for the absorption, N_H (in units of 10^{22} cm^{-2}).

Parameter	A	B	C	A + C (cleaned)	E	F
N_H	20^{+3}_{-3}	13^{+1}_{-1}	17^{+4}_{-2}	19^{+2}_{-2}	$8.2^{+0.8}_{-0.6}$	$6.72^{+0.36}_{-0.34}$
Γ	$1.25^{+0.25}_{-0.23}$	$1.29^{+0.11}_{-0.11}$	$1.47^{+0.35}_{-0.23}$	$1.54^{+0.17}_{-0.22}$	$1.57^{+0.13}_{-0.10}$	$1.11^{+0.06}_{-0.06}$
Unabs. Flux	1.1	6.5	0.7	0.8	0.65	4.4
χ^2_ν/dof	1.035/41	1.130/128	0.690/35	1.085/60	1.008/90	1.196/176

F, reaching a net exposure time of 5085 s. An absorbed power law gave a good fit above 2 keV, but showed some positive residuals (although never exceeding 3 σ from the model) at softer energies (reduced χ^2_ν=1.196 for 176 degrees of freedom, dof, see the upper panel in Fig. 4). These positive residuals suggest the presence of either (1) an additional soft component, (2) an ionized absorber or (3) a partial covering. Thus, we first added a black body component to the power law continuum, obtaining a better fit (reduced χ^2=0.987 for 174 dof; F-test probability of 5.53×10^{-8}). This resulted in a softer and more absorbed power law, and a black body with temperature of 0.17 keV and emitting radius of a few hundred km.

The use of an ionized absorber (ABSORI in XSPEC; Done et al. 1992), in addition to a neutral one accounting for the interstellar absorption (PHABS), also resulted in a better fit with respect to the simple absorbed power law (reduced χ^2=0.950 for 174 dof; F-test probability of 1.99×10^{-9}). The absorber temperature was fixed to 30 kK and the power law photon index of the photoionizing source was linked to the photon index of the continuum. The absorber ionization state ξ (defined as ξ=L/nR^2, where L is the X–ray luminosity of the ionizing source, n is the density of the absorber, and R is the distance of the ionized matter from the X–ray source), resulted in a value of $125\,^{+60}_{-45}$ erg cm s^{-1}.

A better fit with respect to the simple absorbed power law (reduced χ^2_ν=0.971 for 174 dof; F-test probability of 1.335×10^{-8}) was obtained also using a power law continuum modified by a partial covering absorption (PCFABS in XSPEC), together with the usual absorption accounting for the interstellar value. Partial covering parameters are the equivalent hydrogen column density $N_{\rm Hpcfabs}$ and the dimensionless covering fraction, f ($0 < f < 1$). All the best fit parameters of these models are summarized in Table 3. The counts spectra together with their residuals when fitting with three different continua are reported in Fig. 4. The residuals of the partial covering model are not shown because they look very similar to those obtained with the additional soft component (middle panel in Fig. 4). There is no evidence of an iron emission line. Upper limits (95% confidence level) to the equivalent width (EW) of a narrow line from ionized iron (energy fixed at 6.7 keV) can be placed at EW<34 eV, while for a neutral iron emission line (energy fixed at 6.4 keV) at EW<16 eV, assuming a power law continuum.

The overall flares spectrum can be compared with the cumulative spectrum extracted from the 2011 low intensity state (time interval E, average count rate of 0.330 ± 0.005 counts s^{-1}), corresponding to a net EPIC pn exposure of 14.4 ks. An absorbed power law gave a good fit ($\chi^2_\nu = 1.008$ for 90 dof) with the following parameters: $N_{\rm H}$=($8.2^{+0.8}_{-0.6}$)$\times10^{22}$ cm^{-2}, Γ=$1.57^{+0.13}_{-0.10}$. The average observed flux was 3.7×10^{-12} erg cm^{-2} s^{-1}, while the flux corrected for the absorption was 6.5×10^{-12} erg cm^{-2} s^{-1} (1–10 keV), translating into an average luminosity of 1.2×10^{35} erg s^{-1} at 13 kpc. Also an absorbed black body gave a good fit ($\chi^2_\nu = 0.924$ for 90 dof), with $N_{\rm H}$, of $3.6\pm0.4\times10^{22}$ cm^{-2}, a temperature, $kT_{\rm bb}$, of 1.78 ± 0.07 keV and a radius, $R_{\rm bb}$, of 0.29 ± 0.02 km (at 13 kpc). Finally, we fitted the low intensity spectrum with the best fit model obtained for the flares, i.e. an absorbed power law modified with a ionized absorber. This improved the fit quality ($\chi^2_\nu = 0.794$ for 88 dof, F-test probability of 2.75×10^{-5}) and gave the following parameters: $N_{\rm H}$=(4 ± 2)$\times10^{22}$ cm^{-2}, Γ=1.85 $^{+0.20}_{-0.13}$, ionized absorption, $N_{\rm Habsori}$, of (2.5 $^{+0.8}_{-0.6}$) $\times10^{23}$ cm^{-2}, ionization parameter, ξ, of 600 $^{+400}_{-335}$ erg cm s^{-1}. If we fix the ionized absorption parameters $N_{\rm Habsori}$ and ξ values obtained for the cumulative flares spectrum, we again obtain a good fit to the low intensity spectrum ($\chi^2_\nu = 0.886$ for 88 dof), resulting in a column density $N_{\rm H}$=(2.7 $^{+0.7}_{-0.6}$)$\times10^{22}$ cm^{-2} and in a power law photon index Γ=1.7 ± 0.1, consistent with previous results. Therefore, we conclude that the ionized absorber found in the overall flaring spectrum is consistent with being present also during the low intensity emission with similar properties, although the statistics does not permit to be very sensitive to its parameters. In any case, the low intensity emission is softer than the flaring spectrum. The low intensity spectrum fitted with these models is shown in Fig. 5.

Table 3. Spectral results for the cumulative spectrum during flares in time interval F (2011) fitted with models able to account for the soft excess. Flux is in the 1–10 keV energy range in units of 10^{-11} erg cm^{-2} s^{-1} and is corrected only for the absorption N_H (PHABS in XSPEC). Absorbing column densities are in units of 10^{22} cm^{-2}.

Parameter	POW + BB	ABSORI * POW	PCFABS * POW
N_H	$9.41^{+0.48}_{-1.32}$	$0.65^{+0.70}_{-0.50}$	$5.39^{+0.69}_{-0.86}$
$N_{\rm Habsori}$	–	$15.8^{+2.0}_{-1.8}$	–
ξ	–	125^{+60}_{-45}	–
$N_{\rm Hpcfabs}$	–	–	$11.7^{+4.8}_{-3.7}$
f	–	–	$0.59^{+0.12}_{-0.11}$
Γ	$1.33^{+0.08}_{-0.12}$	$1.29^{+0.07}_{-0.07}$	$1.42^{+0.12}_{-0.12}$
$kT_{\rm bb}$ (keV)	$0.17^{+0.02}_{-0.03}$	–	–
$R_{\rm bb}$ (km)	250^{+430}_{-90}	–	–
Unabs. Flux	10.7	3.1	4.0
χ^2_ν/dof	0.987/174	0.950/174	0.971/174

Finally, we also performed an intensity selected spectroscopy: a series of intensity selected spectra were produced, using intervals corresponding to EPIC pn count rates of <1, 1–5, 5–10, and >10 counts s^{-1}, when the data are accumulated with a binning of 256 s,

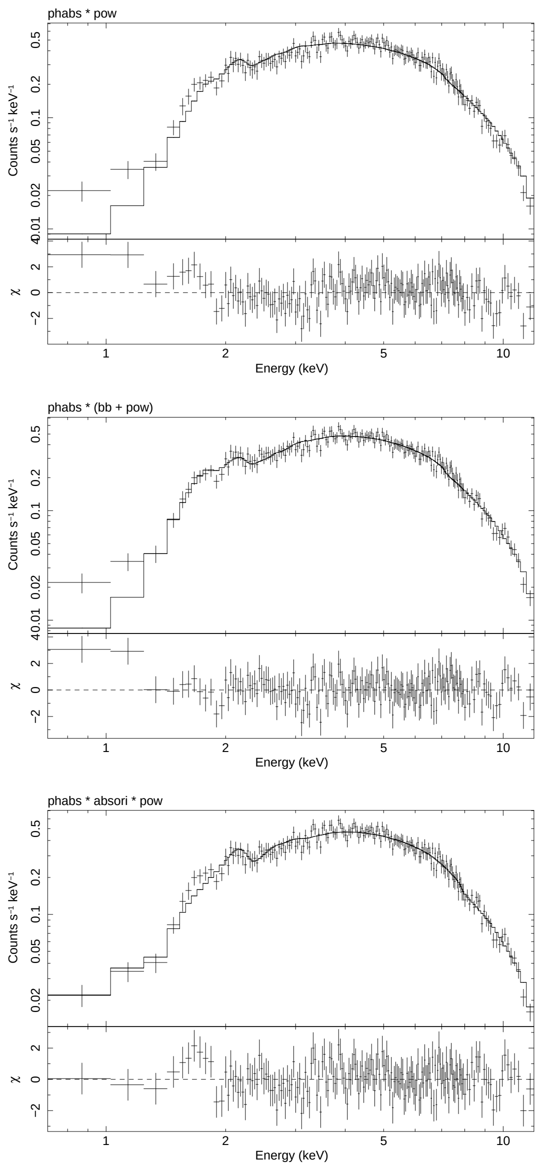

Figure 4. Cumulative X–ray spectrum of the flaring activity of the second part of the 2011 observation (flares in interval F). The *upper panel* shows the counts spectrum together with the residuals (in units of standard deviations) when fitting with an absorbed power law. The *middle panel* shows the residuals when fitting with a power law together with a black body. *Lower panel* displays the residuals when fitting with a power law continuum modified by a ionized absorber (ABSORI in XSPEC, see Sect.3.1 for details).

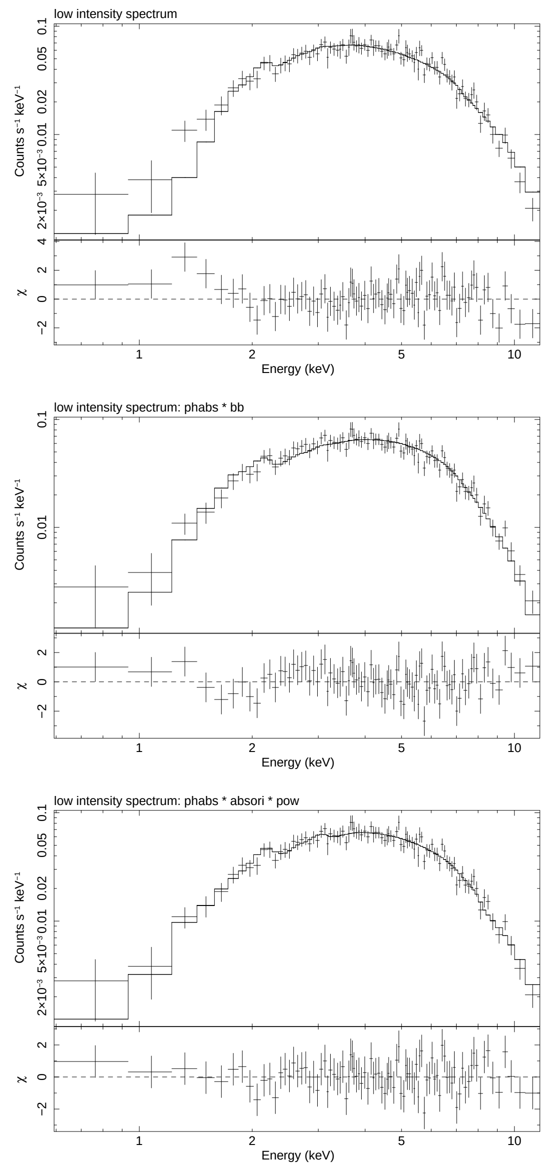

Figure 5. X–ray counts spectra and residuals (in units of standard deviations) for the low intensity emission observed in 2011 (interval E) fitted with an absorbed power law model (*upper panel*), an absorbed black body (*middle panel*), and an absorbed power law modified with a ionized absorber (*lower panel*).

for both observations (2004 and 2011). The best-fit, obtained with an absorbed power law, is reported in Table 4, and it clearly indicates that the spectrum is harder when the source is brighter, as usually observed in accreting pulsars.

3.2 Timing Analysis

For the timing analysis we used both MOS and pn EPIC data. Arrival times were corrected to the Solar System barycenter, but not for the 3.7 days orbital motion, owing to the unknown parameters of the system. The observability of the periodicity at 1246$\pm$100 s (Walter et al. 2006) is complicated by the presence of the strong flares which occur on a comparable time scale. Folding the data of the whole observation at different trial periods produces several peaks in the χ^2 distribution. On the other hand, by restricting the period search to the central part of the 2011 observation (interval E), when the source was in a low intensity and non-flaring state, the X–ray pulsations are clearly detected at a period, P, of 1212$\pm$6 s (χ^2=252, for 9 dof). The corresponding folded light curve is plotted in Fig. 6.

Also in the 2004 observation the source pulsations are more easily detected during the non flaring time interval. By a standard folding analysis of the time interval C we obtained a clear peak in the χ^2 distribution at P = 1216$\pm$7 s (χ^2=257 for 9 dof). Based on this result, we could then refine the period estimate using the data from the whole observation, which gave P = 1213$\pm$2 s. The folded

Table 4. Results of the intensity selected spectroscopy. An absorbed power law model was used. Flux is in the 1–10 keV energy range in units of 10^{-11} erg cm^{-2} s^{-1} and is corrected for the absorption, N_H (in units of 10^{22} cm^{-2}). Uncertainties on the unabsorbed fluxes are about 3%.

Obs. 2004 Parameter	$<$1 c s^{-1}	1–5 c s^{-1}	5–10 c s^{-1}	$>$10 c s^{-1}
N_H	19^{+2}_{-2}	13^{+1}_{-1}		
Γ	$1.54^{+0.17}_{-0.22}$	$1.29^{+0.11}_{-0.11}$		
Unabs. Flux	0.8	6.5		
χ^2_ν/dof	1.085/60	1.130/128		
Obs. 2011 Parameter	$<$1 c s^{-1}	1–5 c s^{-1}	5–10 c s^{-1}	$>$10 c s^{-1}
N_H	$8.2^{+0.8}_{-0.6}$	$6.9^{+0.3}_{-0.3}$	$5.70^{+0.53}_{-0.49}$	$5.60^{+0.50}_{-0.50}$
Γ	$1.57^{+0.13}_{-0.10}$	$1.12^{+0.05}_{-0.05}$	$1.05^{+0.10}_{-0.10}$	$0.88^{+0.09}_{-0.09}$
Unabs. Flux	0.7	5.0	11.7	20.0
χ^2_ν/dof	1.008/90	1.147/209	0.823/119	1.190/137

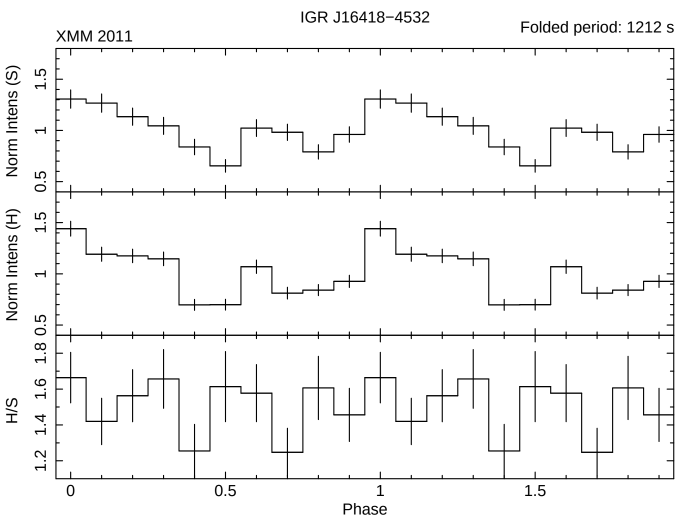

Figure 6. IGR J16418–4532 pulse profiles at soft (0.3–4 keV) and hard energies (4–12 keV) with *XMM-Newton* in 2011 (only the low intensity emission), together with their hardness ratio, obtained folding the light curve at a period of 1212 s. The zero phase is arbitrary.

light curve for the non-flaring time interval is plotted in Fig. 7. Contrary to that obtained in 2011, it shows a single broad peak.

We finally performed a timing analysis of a series of *RXTE*/PCA archival observations carried out between 2009 April 5 and April 15, obtaining a best fit spin period of 1209.4$\pm$1 s. The comparison of the pulse periods measured with *XMM-Newton* in 2004 and 2011 and with *RXTE* in 2009 does not show significant spin-up or spin-down.

4 DISCUSSION

INTEGRAL showed that IGR J16418–4532 is an X–ray transient with frequent flaring activity: it detected source outbursts

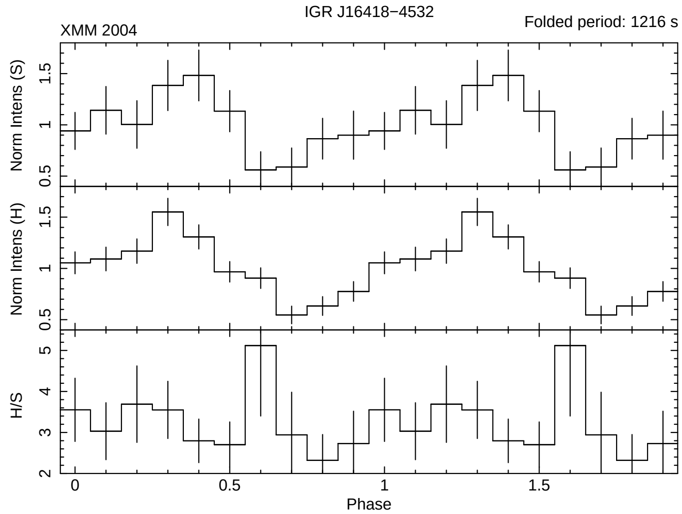

Figure 7. IGR J16418–4532 pulse profiles at soft (0.3–4 keV) and hard energies (4–12 keV) with *XMM-Newton* in 2004 (only the low intensity emission), together with their hardness ratio, obtained folding the light curve at a period of 1216 s. The zero phase is arbitrary.

above 10^{-10} erg cm^{-2} s^{-1} (20–100 keV) for about 1% of the *INTEGRAL* total exposure time of the source region (Ducci et al. 2010). This led to suggest IGR J16418–4532 as a member of the class of the supergiant fast X–ray transients (SFXTs, Sguera et al. (2006); see Sidoli (2010) for an updated review of the SFXTs properties). It has been classified as a "candidate" SFXT because the supergiant nature of its optical counterpart has not been confirmed yet, and the X–ray dynamic range was not as extreme as the prototypical SFXTs (typically, from 3 to 5 orders of magnitudes in X–ray intensity). Among SFXTs, IGR J16418–4532 is, after IGR J16479–4514 and IGR J18483–0311, the source with the most frequent bright flaring activity (Ducci et al. 2010, Sidoli 2010).

Our *XMM-Newton* observation allowed us to continuously follow the source variability with unprecedented detail and to reveal, for the first time in this source, a wide dynamic range, typical of other so-called "intermediate" SFXTs, like e.g. IGR J18483–0311 (Sguera et al. 2007) or IGR J16465-4507 (Clark et al. 2010).

The X–ray light curve observed in 2011 showed two episodes of bright flaring activity (exceeding 10 counts s^{-1} in the first part of the exposure), separated by an interval of low intensity emission, where the source faded to less than $\sim$0.1 counts s^{-1} (Fig. 8, middle panel). The two flaring intervals (D and F) were characterized by different variability patterns: in the first one the flux reached the peak during the longest flare ($\sim$4000 s) and showed a variety of flare shapes, while in interval F the flares had a more regular appearance, with a hint of a quasi–periodic pattern of a few ks, not related with the long spin period (see the lower panel of Fig. 8). A quasi–periodic flaring was also present in the central part of the 2004 observation (time interval B in Fig. 1). As visible in the upper panel of Fig. 8, the variability consisted of two sub-sets of four flares each, recurring every $\sim$380–400 s.

Quasi–periodic flares have been seen also in other HMXBs, including some SFXTs (e.g. XTE J1739–302, see Ducci et al. 2010). For example, in the Be/X-ray transient EXO 2030+375 flares recurring on timescales of 3.96$\pm$0.04 hr, and intensity oscillations with periods of 900-1200 s, were observed and explained

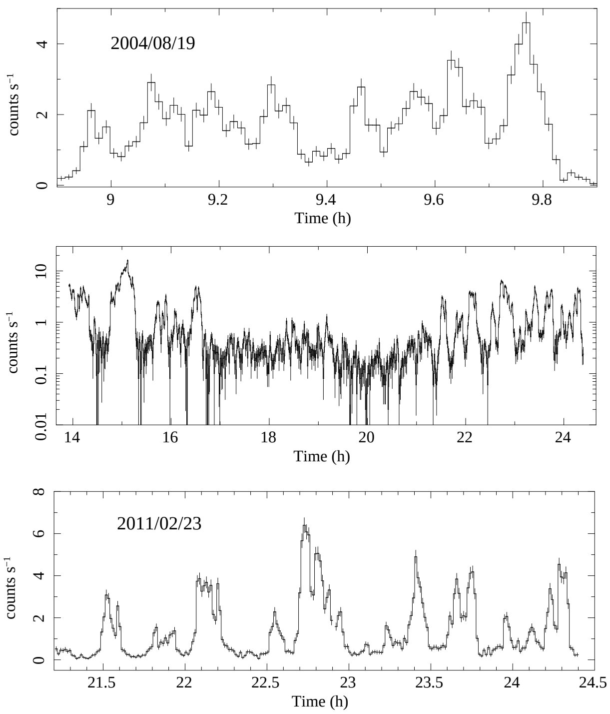

Figure 8. Close-up views of IGR J16418–4532 light curves shown in Fig. 1. In the *middle panel* we show the 2011 light curve (same as in Fig. 1) in logarithmic scale to more clearly show the high dynamic range now observed in IGR J16418–4532. In the *upper* and *lower panels* two close-up views of the 2004 and 2011 observations are displayed, respectively, to better show the time intervals where quasi-periodic flaring activity is present.

with the formation and disruption of a temporary and transient accretion disk around the neutron star (Parmar et al. 1989). Although in EXO 2030+375 both the flare shapes (well described by a fast rise and an exponential decay) and the time recurrence were more regular, it is possible that a similar mechanism is responsible for the IGR J16418–4532 flaring activity. The model proposed by Taam et al. (1988) predicts that similar recurrence time scales for the flares can be well reproduced by a relative velocity of the neutron star with respect to the outflowing wind of about 1200–1400 km s^{-1} (see also Ducci et al. 2010 and references therein).

We note a striking similarity between the IGR J16418–4532 light curve observed in 2011 and the prediction of hydrodynamic simulations for systems accreting in the so-called "transitional case" between "pure" wind accretion and "full" Roche lobe overflow (Blondin & Owen 1997). According to these simulations, in this particular transitional accretion regime, when the mass donor is close to fill its Roche lobe, the HMXB can display an X–ray light curve very similar to what we observed in IGR J16418–4532, both for what concerns the variability time scale and its dynamic range (see Fig. 8, middle panel). The mass loss from the supergiant is dominated by the strong wind, but with the additional contribution of a weak tidal gas stream, focussed towards the neutron star (hereafter, NS). This mechanism produces extreme variations in the mass accretion rate, mainly due to the dynamical interaction of the weak tidal gas stream with the accretion bow shock around the NS (Blondin & Owen 1997). We are aware that these simulations have been performed in two dimensions (computing the gas flow within the orbital plane) and the real 3D case is much more complex, but nevertheless we think that the similarity with the observed light curve deserves attention and further investigation.

Similarly, Bhattacharya & van den Heuvel (1991) discussed the case of HMXBs with short orbital periods (P$\leqslant$3-4.5 days), such as IGR J16418–4532, as sources where the orbits are typically narrow making accretion via "beginning atmospheric Roche-lobe overflow" an attainable mechanism to produce X–ray emission. In general, under the assumption that a supergiant star has a sharply defined radius (e.g. the photospheric radius), Roche lobe overflow starts as soon as such radius extends beyond the Roche lobe. However, in reality the supergiant star does not have a sharp edge or radius and above its photosphere there is still atmospheric material in the form of strong stellar wind. Consequently, already before the photospheric radius reaches the Roche lobe, a small part of the stellar wind can begin to flow towards the neutron star through the inner Lagrangian point. In principle, this could also favour the formation of a transient and temporary accretion disk whose disruption could produce the observed quasi-periodic flares from IGR J16418–4532.

Given the short orbital period of 3.7389 days, we plot in Fig. 9 the Roche lobe radius of the companion star at periastron, as a function of its mass and for different system eccentricities (Eggleton 1983). The radii of massive early type stars of different luminosity classes (Vacca et al. 1996) are also plotted for comparison. The 32.8 kK best fit effective temperature[3] of the candidate counterpart (Rahoui et al. 2008) indicates a O8.5–O9.5 type star, which can be in a narrow circular orbit with the NS, avoiding Roche lobe overflow. For example, a O9 Ia (O8.5 Ia) star with a mass of 46 $M_\odot$ (50 $M_\odot$) and a radius of 24 $R_\odot$ (Vacca et al. 1996) in a circular orbit is consistent with the optical and X–ray observations. Another viable possibility is a O9.5 III companion with a mass of 24 $M_\odot$ and a radius of $\sim$15 $R_\odot$. In this case the eccentricity can range from e=0 to e$\sim$0.2 without exceeding the Roche lobe surface. We are aware that the above speculations on the optical counterpart are rather uncertain in the lack of an optical spectrum, but we here only note that an early type supergiant (and a SFXT nature) is compatible with the short orbital period. Moreover, a narrow orbit in a massive binary is required in the "transitional case" we suggested above to explain IGR J16418–4532 properties.

Comparison of the 2011 spectral results with the previous XMM-$Newton$ observation shows a lower absorbing column density in 2011 than in 2004. However, in both occasions, the absorption was well in excess with respect to the total Galactic column density towards the source. It is possible that the variability of the absorption in the two observations is due to the different orbital phases covered by the two observations, but the uncertainties on the orbital parameters do not allow us to determine the absolute orbital phase covered by two spectra. The local absorbing column density due to the supergiant wind in a HMXBs is expected to vary along the orbit, even in case of a spherically symmetric wind, also in dependence of the inclination of the system. Further variability can be due to the presence of different gas structures (accretion wake around the NS together with tidal effects which induce a gas stream from the supergiant) which form because of the presence of the NS gravitational field (Blondin et al. 1991).

Another important result is that the possible hint for a soft excess present in 2004, is now well established by the 2011 observation and it is compatible with the presence of a ionized absorber. In particular, the cumulative X–ray spectrum during the flares ob-

[3] with very large uncertainties: $T_{\rm eff}$ can range from 36 kK to 10.6 kK

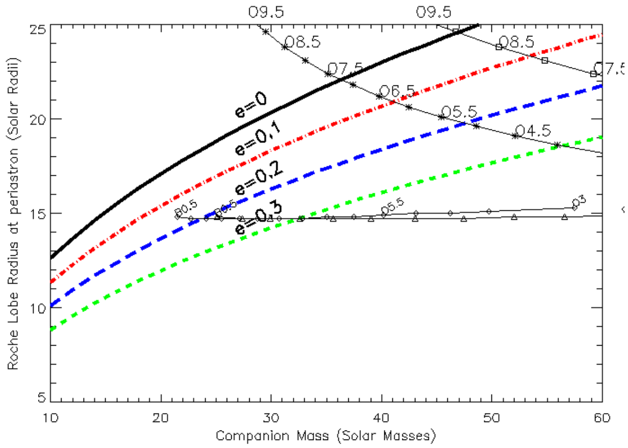

Figure 9. Roche lobe radius at periastron versus the companion mass, assuming an orbital period of 3.7389 days, and different eccentricities. We overplot also the radii of early type stars, taken from Vacca et al. (1996): diamonds and triangles mark OB star with luminosity class III, their spectroscopic and evolutionary masses, respectively (Table 6 in Vacca et al. 1996), while asterisks and open squares mark supergiant stars (data are from Table 7 in Vacca et al. 1996), their spectroscopic and evolutionary masses, respectively, for different spectral types.

served in 2011 (F) is well described introducing an additional ionized absorber, resulting in an absorber ionization state, ξ, of 125 $^{+60}_{-45}$ erg cm s^{-1}, and an absorbing column density, $N_{\rm Habsori}$, of $15.8^{+2.0}_{-1.8}\times10^{22}$ cm^{-2}. In the likely hypothesis of the wind photoionization, the above value of the ionization parameter ξ indicates, for example, the presence of highly ionized oxygen (O VIII) and neon (Ne X ions) (Kallman & McCray 1982), whose lines could have been observed in the RGS energy range, if the source had been brighter and less absorbed. The average X–ray flux during flares, corrected for both interstellar and local (ionized) absorption is 5×10^{-11} erg cm^{-2} s^{-1} (1–10 keV), which implies a ionizing X–ray luminosity L=10^{36} erg s^{-1}. Although the ξ value we obtained is very likely an average value, it is possible to calculate the distance, R, from the X–ray source of the main component of the absorbing ionized material. Using the measured $N_{\rm Habsori}$ value and assuming $N_{\rm Habsori}$ = nR, we obtain a distance R=5×10^{10} cm, which is compatible with the NS accretion radius, and well within the orbital separation ($\sim10^{12}$ cm) of the binary system.

5 CONCLUSION

The new *XMM-Newton* observations we have reported here allowed us to perform an in-depth investigation of the transient source IGR J16418–4532. A high dynamic range has been observed for the first time, of about two orders of magnitude, leading to a firmer classification of IGR J16418–4532 as a member of the class of the SFXTs.

We obtained a more precise value of the pulse period and we clearly established the presence of a soft X–ray excess in the flares X–ray spectrum, which we interpreted as due to the presence of ionized wind material, mainly located at a distance compatible with the NS accretion radius. The absorbing column density variations between 2004 and 2011 are likely due to the different orbital phases covered between the two observations. The low intensity emission is both softer and more absorbed than during bright flares.

The kind of X–ray variability (its high dynamic range on the observed time scale), together with the candidate optical counterpart, the short orbital period and the quasi-periodic flaring activity, all suggest that the X–ray emission from IGR J16418–4532 is driven by a transitional accretion regime, intermediate between “pure” wind accretion and “full” Roche lobe overflow.

In conclusion, we suggest here for the first time that this hypothesis could explain both IGR J16418–4532 X–ray behaviour and possibly other SFXTs with similarly short orbital periods.

ACKNOWLEDGMENTS

This work is based on data from observations with *XMM-Newton*. *XMM-Newton* is an ESA science mission with instruments and contributions directly funded by ESA Member States and the USA (NASA). We thank the *XMM-Newton* duty scientists and science planners for making these observations possible, in particular Rosario Gonzalez-Riestra (*XMM-Newton* Science Operations Centre User Support Group). Lara Sidoli thanks John Blondin for interesting discussions. We made use of HEASARC online services, supported by NASA/GSFC. This work was supported by the grant from PRIN-INAF 2009, “The transient X–ray sky: new classes of X–ray binaries containing neutron stars” (PI: L. Sidoli).

REFERENCES

Bhattacharya D., van den Heuvel E. P. J., 1991, Phys. Reports, 203, 1

Blondin J. M., Owen M. P., 1997, in D. T. Wickramasinghe, G. V. Bicknell, & L. Ferrario ed., IAU Colloq. 163: Accretion Phenomena and Related Outflows Vol. 121 of Astronomical Society of the Pacific Conference Series, Wind Accretion VS Roche Lobe Overflow in HMXBs. pp 361–+

Blondin J. M., Stevens I. R., Kallman T. R., 1991, ApJ, 371, 684

Chaty S., Rahoui F., Foellmi C., Tomsick J. A., Rodriguez J., Walter R., 2008, ArXiv e-prints 0802.1774

Clark D. J., Sguera V., Bird A. J., McBride V. A., Hill A. B., Scaringi S., Drave S., Bazzano A., Dean A. J., 2010, MNRAS, 406, L75

Corbet R., Barbier L., Barthelmy S., Cummings J., Fenimore E., Gehrels N., Hullinger D., Krimm H., Markwardt C., Palmer D., Parsons A., Sakamoto T., Sato G., Tueller J., Remillard R., 2006, The Astronomer’s Telegram, 779, 1

den Herder J. W., Brinkman A. C., Kahn S. M., Branduardi-Raymont G., Thomsen K., Aarts H., Audard M., Bixler J. V. e. a., 2001, A&A, 365, L7

Dickey J. M., Lockman F. J., 1990, ARA&A, 28, 215

Done C., Mulchaey J. S., Mushotzky R. F., Arnaud K. A., 1992, ApJ, 395, 275

Ducci L., Sidoli L., Paizis A., 2010, MNRAS, 408, 1540

Eggleton P. P., 1983, ApJ, 268, 368

Kallman T. R., McCray R., 1982, ApJS, 50, 263

Levine A. M., Bradt H. V., Chakrabarty D., Corbet R. H. D., Harris R. J., 2011, ApJS, 196, 6

Parmar A. N., White N. E., Stella L., 1989, ApJ, 338, 373

Rahoui F., Chaty S., Lagage P.-O., Pantin E., 2008, A&A, 484, 801

Romano P., Mangano V., Esposito P., Kennea J. A., Evans P. A., Vercellone S., Burrows D. N., Chester M. M., Cusumano G.,

Farinelli R., Krimm H., La Parola V., 2011, The Astronomer's Telegram, 3174, 1
Sguera V., Bazzano A., Bird A. J., Dean A. J., Ubertini P., Barlow E. J., Bassani L., Clark D. J., Hill A. B., Malizia A., Molina M., Stephen J. B., 2006, ApJ, 646, 452
Sguera V., Hill A. B., Bird A. J., Dean A. J., Bazzano A., Ubertini P., Masetti N., Landi R., Malizia A., Clark D. J., Molina M., 2007, A&A, 467, 249
Sidoli L., 2010, in 25th Texas Symposium on Relativistic Astrophysics Supergiant Fast X-ray Transients, (arXiv:1103.6174)
Strüder L., Briel U., Dennerl K., Hartmann R., Kendziorra E., Meidinger N., Pfeffermann E., Reppin C., et al. 2001, A&A, 365, L18
Taam R. E., Brown D. A., Fryxell B. A., 1988, ApJL, 331, L117
Tomsick J. A., Lingenfelter R., Corbel S., Goldwurm A., Kaaret P., 2004, The Astronomer's Telegram, 224, 1
Turner M. J. L., Abbey A., Arnaud M., Balasini M., Barbera M., Belsole E., Bennie P. J., Bernard J. P., et al. 2001, A&A, 365, L27
Vacca W. D., Garmany C. D., Shull J. M., 1996, ApJ, 460, 914
Walter R., Zurita Heras J., Bassani L., Bazzano A., Bodaghee A., Dean A., Dubath P., Parmar A. N., Renaud M., Ubertini P., 2006, A&A, 453, 133
Wilms J., Allen A., McCray R., 2000, ApJ, 542, 914

This paper has been typeset from a TEX/ LATEX file prepared by the author.